HHS Public Access

Author manuscript

Nat Neurosci. Author manuscript; available in PMC 2020 May 11.

Published in final edited form as:

Nat Neurosci. 2019 December ; 22(12): 2078–2086. doi:10.1038/s41593-019-0523-z.

Memory retrieval modulates spatial tuning of single neurons in the human entorhinal cortex

Salman E. Qasim[1], **Jonathan Miller**[1], **Cory S. Inman**[2], **Robert E. Gross**[2], **Jon T. Willie**[2], **Bradley Lega**[3], **Jui-Jui Lin**[3], **Ashwini Sharan**[4], **Chengyuan Wu**[4], **Michael R. Sperling**[5], **Sameer A. Sheth**[6], **Guy M. McKhann**[7], **Elliot H. Smith**[8], **Catherine Schevon**[9], **Joel M. Stein**[10], **Joshua Jacobs**[*,1]

[1]Department of Biomedical Engineering, Columbia University, New York, NY 10027

[2]Department of Neurological Surgery, Emory University, Atlanta, GA 30322

[3]Department of Neurological Surgery, University of Texas Southwestern, Dallas, TX 75390

[4]Department of Neurological Surgery, Thomas Jefferson University, Philadelphia, PA 19107

[5]Department of Neurology, Thomas Jefferson University, Philadelphia, PA 19107

[6]Department of Neurological Surgery, Baylor College of Medicine, Houston, TX, 77030

[7]Department of Neurological Surgery, Columbia University, New York, NY 10032

[8]Department of Neurosurgery, University of Utah, Salt Lake City, UT 84132

[9]Department of Neurology, Columbia University, New York, NY 10032

[10]Department of Radiology, University of Pennsylvania, Philadelphia, PA 19104

Abstract

The medial temporal lobe (MTL) is critical for both spatial navigation and memory. While single neurons in the MTL activate to represent locations in the environment during navigation, it remains unclear how this spatial tuning relates to memory for events involving those locations. We examined memory-related changes in spatial tuning by recording single-neuron activity from neurosurgical patients performing a virtual-reality object-location memory task. We identified "memory-trace cells" whose activity was spatially tuned to the retrieved location of the specific object that subjects were cued to remember. Memory-trace cells in the entorhinal cortex (EC), in particular, encoded discriminable representations of different memories through a memory-

[*]Correspondence: joshua.jacobs@columbia.edu, 351 Engineering Terrace, Mail Code 8904, 1210 Amsterdam Avenue, New York, NY 10027, 212-854-2445.

Author contributions

J.J. conceived the experiment, R.E.G., J.T.W., B.L., A.S., C.W., S.A.S., G.M.M. performed surgical procedures, S.E.Q., J.M., M.R.S., C.S., E.H.S., J.J.L., C.S.I., performed data collection and recording, J.M.S. processed neuroimaging data, S.E.Q. analyzed the data, S.E.Q. and J.J. wrote the manuscript.

Competing interests

The authors declare no competing interests.

specific rate code. These findings indicate that single neurons in the human EC change their spatial tuning to target relevant memories for retrieval.

Introduction

A key feature of memory is our ability to selectively recall particular experiences even if they occurred in a setting shared with other events. For example, if asked to recommend a tourist itinerary for a city you visited frequently, you can selectively recall distinct memories of locations from different trips to provide an answer. While lesion studies have demonstrated that many declarative memory processes depend on intact medial temporal lobe structures, such as the hippocampus and entorhinal cortex (EC)[1,2], it is not clear how neuronal activity in these regions enables us to target a particular memory for retrieval among related experiences.

We examined how the brain represents distinct memories through the lens of spatial cognition, relying on the fact that the brain uses similar circuits and mechanisms to support both spatial and memory processes[3,4]. The discoveries of place cells in the hippocampus[5] and grid cells in the EC[6] demonstrated that neurons in these memory-critical regions[2] also exhibit spatial tuning. Previous work proposed that spatially tuned cells remap their firing patterns across different environments, so events that occur in different environments are associated with different spatial maps[7, 8]. Recent work has extended this idea that different contexts are associated with different spatial maps by showing that the activity of spatially tuned cells may be modulated by changes to internal, top-down processes such as an animal's behavioral state, attention, or goal[9–11]. In this way, different patterns of spatially modulated neuronal activity may index different behavioral and cognitive contexts, and these distinct neural representations may aid in the retrieval of distinct memories.

The EC is a viable candidate for linking memory retrieval to spatial representation[12], as it features a variety of spatially tuned cells[6, 13], plays a role in memory maintenance and retrieval[14, 15], and integrates diverse sensory and cognitive information about an experience in service of memory[16, 17]. Recent work has begun to link memory processes with spatial firing patterns in the EC, such as the identification of "object-trace" cells in the rodent EC whose spatial tuning was determined by the locations previously occupied by objects[18], the finding of reduced grid-cell representations in patients at risk for Alzheimer's disease[19], and the discovery that remembered reward locations influence grid-cell field locations[20].

Building off this work, we hypothesized that single neurons in the MTL, and particularly in the EC, would exhibit spatial tuning modulated by past experiences. Such separable neuronal representations may, in turn, enable top-down, targeted memory retrieval of those past experiences. To test this hypothesis, we analyzed the activity of single neurons from the MTL of human epilepsy patients as they performed a cued spatial-memory task in which they learned and subsequently recalled object locations while moving through a virtual environment. A key feature of this task is that subjects were provided a cue on each trial denoting the specific object location to retrieve, while the environment remained unchanged —this enabled us to assess how top-down, targeted memory retrieval might engage distinct spatial representations in the brain. We observed single neurons, largely in the EC, whose

spatial tuning varied as a function of the particular cue provided for memory retrieval. Specifically, the activity of these cells tracked the patients' subjective memory for the current cued object location, hence we refer to them as "memory-trace" cells. Furthermore, the firing of EC memory-trace cells showed a memory-specific rate code that distinguished which object-location memory had been cued for retrieval. This memory-specific rate code was robust, emerging both when subjects were near the cued objects' location, as well as when subjects were provided with a retrieval cue but did not move through the environment. These findings illustrate how spatially tuned neurons in the EC support our ability to use top-down cues to selectively target relevant memories for retrieval.

Results

We recorded from 299 neurons in the EC, hippocampus, amygdala, and cingulate cortex of 19 neurosurgical patients who performed an object-location memory task (Fig. 1a, Supplementary Figs. 1,2). In this task, subjects were instructed to learn the locations of different objects along a virtual linear track and then to recall the locations after the objects were removed. The task consisted of separate encoding and retrieval trials, which followed the same general structure, except that objects were visible on the track during encoding and absent during retrieval trials. Each trial began with an "instruction period," in which subjects viewed the name of the cued object for that trial. The "hold period" followed, during which subjects remained stationary at the entrance to the track for 4 seconds. Next was the "movement period", in which the subject was moved automatically down the track at randomly varying speeds. During encoding trials, the object was present on the track, enabling the subject to press a button as they reached the object's visible location (Fig. 1b). During retrieval trials, the object was absent and the subject pressed a button at the location where they remembered the cued object being present (Supplementary Video 1). Subjects generally showed high accuracy during retrieval trials, pressing the button within 2.8 virtual units (VR-bins) of the correct location, or 7% of the track length, on average (Fig. 1c).

We examined how the activity of individual neurons (see Fig. 1d for example) represented the subjects' spatial location in the task by computing each neuron's firing rate as a function of their position along the track during retrieval trials. To assess the modulation of neuronal activity, we used a two-way repeated-measure ANOVA to identify neurons whose activity during retrieval trials varied as a function of the subject's location (1 – 40 spatial bins), the retrieval cue (1 – 4 possible cues), and their interaction, determining significance using a permutation procedure. As we describe below, this analysis revealed two groups of neurons with distinct firing patterns (Fig. 2). We found neurons with firing rates that varied as a function of only subject location, similar to conventional place cells[5, 21]. We also found neurons, that we refer to as memory-trace cells, whose spatial tuning shifted along the track depending on the retrieval cue that the subject had viewed at the beginning of each trial.

Place cells activate in fixed locations, independent of memory retrieval demands.

We identified place cells as those that showed a significant main effect of location on firing rate, and had at least one place field (Fig. 3; see Methods). A significant number of cells (50 of 299, $p = 8.78 \times 10^{-14}$, binomial test vs. 5% chance) fulfilled our criteria as place cells.

Most place fields were smaller than 10% of the track length and none covered more than 40% of the track (Fig. 3c).

We found significant numbers of place cells in the EC, hippocampus, and cingulate (Fig. 3d; all p's$< 10^{-4}$, binomial test vs. 5% chance). To examine the possibility that these findings were the result of neuronal responses to time[22] or speed[23], we used an ANCOVA to test if these cells' location-related modulation persisted after including speed and time as covariates[24]. 90% of place cells still exhibited significant spatial coding after accounting for potential effects of time or speed, indicating that their activity primarily reflected the subject's spatial location.

Spatial tuning of memory-trace cells shifts according to the retrieval cue.

In contrast to place cells, Figure 2b depicts the activity of two example EC memory-trace cells, whose spatial tuning shifted depending on the particular object–location cue that the subject viewed at the beginning of each trial. We identified memory-trace cells systematically as those cells that showed significantly increased firing in contiguous spatial bins for at least one cue, which we refer to as "trace fields" (see Methods), and whose spatial firing pattern significantly shifted across different cues (determined via a location × cue interaction in the ANOVA). Overall, a significant number of cells (43 of 299; $p = 6.37 \times 10^{-10}$, binomial test vs. 5% chance) fulfilled these criteria for memory-trace cells (Supplementary Figs. 3,4). These cells were found primarily in the entorhinal and cingulate cortices (Fig. 4a; p's$< 10^{-5}$, binomial tests vs. 5% chance). We observed at least one memory-trace cell in 15 of 19 subjects (Supplementary Table 1); 12 of 19 subjects exhibited both place and memory-trace cells.

Individual memory-trace cells exhibited a unique trace field for anywhere between one and four cues (Fig. 4b, see Supplementary Fig. 4), distinguishing them from "cue-association" cells[25] which only responded to a single association. Specifically, the firing of many memory-trace cells shifted to represent multiple locations over the course of a session, often appearing to fire near the location of the object cued for each trial.

To determine if memory-trace-cell activity reflected underlying memory retrieval processes, we next examined whether the spatial tuning of these neurons was more strongly anchored to the response location—where the subject believed the object to be—rather than the object's true location[26]. If this were the case then re-aligning memory-trace cell firing relative to the response location would yield a stronger pattern of spatially modulated firing compared to the pattern observed when re-aligning firing rate relative to the object location. We tested this by quantifying the spatial information[27], a measure of the specificity of the spatial tuning, in both the response- and object-aligned configurations for each of the four cues. Spatial information was significantly greater in the response-aligned configuration compared to the object-aligned configuration (Fig. 4c, sign-rank test, $z = 3.4$, $p = 0.0007$), suggesting that memory-trace cell firing represents subjects' location relative to the location targeted for memory retrieval.

Memory-trace cell activity tracks subjective memory for cued object locations during retrieval.

Having determined that memory-trace cells were more strongly spatially tuned in response-aligned configurations, we next assessed in more detail where these cells fired in relation to the location of subjects' responses. As shown in Figure 5a, trace fields clustered in the spatial bins immediately preceding the response, appearing on average 2.5 VR-bins before the response location ($t(125) = -2.09$, $p = 0.038$). This suggested that trace-field activity signaled the relevance of a location for upcoming memory retrieval[28]. Furthermore, trace fields appeared significantly closer to subjects' response locations than the true object location on a given trial ($t(1495) = 1.79$, $p = 0.037$). To confirm this preference for locations preceding the response, we computed the grand average of memory-trace cell firing rates in the spatial locations surrounding the response (Fig. 5b). This confirmed that memory-trace cells generally increased their firing as subjects approached the response location, and then decreased following the response (paired *t*-test pre- vs. post-firing rate, $t(1986)=3.99$, $p = 6.73 \times 10^{-25}$; Supplementary Fig. 5). The broad peak and gradual decline in average firing rate across memory-trace cells depicted in Figure 5b reflects the heterogeneity of trace-field offsets relative to the response location (Fig. 5a), as opposed to all trace fields appearing at the same offset.

To further test if memory-trace cell activity tracks subjective memory we analyzed the memory-trace cell firing rate on retrieval trials where subjects made large errors (16.8 % of trials)—these trials enabled us to dissociate subjects' response location and the actual object location. By comparing the response- and object-aligned firing rates during these trials, we found that these cells' firing peaked significantly closer to the response location than the actual object location (Fig. 5c; $t(333) = 2.13$, $p = 0.033$). These results further support the notion that memory-trace cell spatial tuning is anchored to subjects' retrieval of a cued object's location from memory.

Because cells in the MTL have shown evidence of coding for time[22], we considered the possibility that memory-trace cells were firing at specific timepoints, rather than spatial offsets, relative to the response (Supplementary Fig. 6). We thus performed an analysis comparing the degree to which individual memory-trace cell activity was predicted as a function of distance or time relative to the response. This analysis revealed that the firing rates of memory-trace cells were more strongly predicted by the spatial rather than temporal offset ($t(42) = 2.35$, $p = 0.024$), supporting the notion that memory-trace cell activity represents the distance to upcoming recalled locations.

We next sought to better understand the type of distance-to-memory information represented by memory-trace cells. We examined whether memory-trace cell firing fields appeared at fixed offsets from the response location, as might be expected from a general distance code for relevant locations[11], or if they appeared at cue-specific distances, as might be expected in a form of goal-oriented remapping[10]. We conducted an analysis of trace-field offset consistency across cues (Supplementary Fig. 7), and found that a significant number of memory-trace cells had trace fields at reliably fixed offsets across cues (5/37 cells with > 1 trace field, $p = 0.036$, binomial test vs. 5% chance) while a different subset of cells that were equally prevalent (5/37 cells) showed significantly variable offsets across cues.

To further determine if the activity of memory-trace cells specifically relates to memory retrieval, we examined their firing patterns on encoding trials where the cued object was visible. Comparing neural activity between encoding and retrieval trials—which were perceptually identical aside from the visible object—specifically enabled us to identify features of memory-trace cell responses that related to memory retrieval, while controlling for other factors that differed across trials, such as object identity[16], goal locations[11,29], and motor planning[30]. Overall, we found that when a subject was located in a memory-trace cell's firing field, there was increased activity on retrieval trials compared to encoding ($t(125) = 12.9$, $p = 8.9 \times 10^{-24}$; Figs. 5d,e). To assess whether memory-trace cells simply fired in the same locations during encoding trials but with lower firing rates, we computed the spatial correlation between the memory-trace cell firing patterns during retrieval and encoding (*see* Methods, Supplementary Fig. 8). Memory-trace cell spatial firing patterns were largely uncorrelated between encoding and retrieval ($\chi^2(1) = 149.35$, $p < 2.2 \times 10^{-16}$), meaning that the spatial timing we observed during retrieval was not present at lower firing rates during encoding. In contrast, place cells exhibited significantly more stable spatial tuning between encoding and retrieval trials than memory-trace cells (Supplementary Fig. 9; Mann-Whitney U-test, $z = 5.25$, $p = 1.48 \times 10^{-7}$). These results indicate that during encoding memory-trace cells either shift spatial tuning or are simply inactive, supporting the idea that the memory-trace cell spatial tuning we observed uniquely supports memory retrieval. Furthermore, we found no effect of low versus high measures of attention on memory-trace cell activity (*see* Methods, $F_{(1,639)} = 0.16$ & 0.48; p's> 0.05, permutation test), indicating that attention likely did not explain the encoding–retrieval differences. This is consistent with findings indicating that attentional mechanisms do not fundamentally differ between encoding and retrieval[31].

In sum, memory-trace cell spatial tuning was predominantly modulated by subjects' response location specifically during cued memory retrieval. This pattern was robust even when subjects' responses were inaccurate, suggesting that memory-trace cells tracked subjects' internal representation of the cued object's location.

Activity of memory-trace cells in EC separably and robustly represents different memories.

Although the above analyses showed that the activity of memory-trace cells tracked retrieved locations in the environment, it remained unclear whether these cells support memory representations more generally beyond moving through the relevant environment. Understanding this could help explain how we are able to remotely recall events from outside the environment in which they occurred. We investigated this question by analyzing memory-trace cell activity during the hold period of our task, which follows the subjects' initial viewing of the retrieval cue during the instruction period. We hypothesized that during the hold period subjects would exhibit similar neural representations of the current memory retrieval cue as when moving through the target location in the environment. We therefore asked if the same patterns of neuronal activity associated with retrieval of particular memories during movement also emerged during the hold period. Overall, memory-trace cell firing rates were significantly elevated during the hold period of retrieval trials (Fig. 6a; $F_{(4,10075)} = 2.88$, $p = 0.021$, post-hoc t-tests, p's< 0.05, FDR-corrected). This effect was not seen during encoding trials, or by non-trace cells (Supplementary Fig. 10). This indicates

that memory-trace cells were generally engaged during the hold period, even though subjects were still, rather than moving through the environment.

We hypothesized that memory-trace cell activity during the hold period would be correlated with their activity when subjects remembered the location during movement. This correlation might indicate that memory-trace cell representations for retrieved locations generalized beyond memory retrieval during movement, supporting the potential utility of such representations for retrieval across multiple contexts. To facilitate comparison of memory-trace-cell firing rates across the hold period and the response location, we first characterized the changes in firing rate in the spatial bins surrounding the response location (Fig. 5b), which we called the “response period”. We measured the magnitude of the response-modulated changes in memory-trace cell activity by normalizing each cell’s pre-response firing rate by its post-response firing rate. This accounted for the background activity of each neuron and helped ensure that correlations computed between a trial’s hold and response periods would not be confounded by overall trial-wide increases in firing rate. For each cell, we then computed the correlation across trials between the firing rates during the hold and response periods (Fig. 6b). We compared this measure to the correlation in firing rate between the hold period and a matched “control period”, which did not include the response (*see* Methods). We found that memory-trace-cell firing was positively correlated between the hold and response periods, and not between the hold and control periods (Fig. 6c, Supplementary Fig. 11a), indicating that a consistent pattern of neuronal activity for individual cues was present during the hold and response periods (see Fig. 6d and Supplementary Fig. 11b for examples). Firing rates during these periods were not correlated with task performance (Supplementary Fig. 12).

We next used a multivariate cross-decoding analysis[32] to more fully characterize how the neural representations of specific memories that emerged during the response period were recapitulated across various task periods (see Methods; Supplementary Fig. 13). Here we trained separate decoders to predict the currently cued object location memory from the normalized firing rates of the population of memory-trace cells for each task period. We then tested each model’s decoding performance on activity from the response period. In this analysis, if we were to observe that a model trained on one period demonstrated elevated decoding performance when tested on memory-trace-cell firing during the response period, then it would indicate that the neural representations of specific memories were similar between these two periods.

The results of this analysis indicated that the firing rates of EC memory-trace cells, specifically, represented individual memory cues similarly between the hold and response periods. For EC memory-trace cells, when comparing test performance in the response period for various training models, only the model trained on the hold period showed significantly elevated accuracy (Fig. 7a; $p = 0.0043$, binomial test vs. 25% chance). This pattern was not present for memory-trace cells outside the EC (Fig. 7b). Additionally, we observed significant decoding from EC memory-trace cells when we both trained and tested models on the response period using 10-fold cross-validation (white bar, Fig. 7a; $p = 0.029$, binomial test), which confirms the reliability of these patterns. To characterize the patterns of memory-related neural activity across the task more fully, we also performed a complete

cross-decoding analysis, in which we compared the performance of training and testing models across all pairs of task periods (Supplementary Fig. 14c). In particular, we did not find significant cross-decoding for data from the control period. This indicates that EC memory-trace cells do not represent the currently cued memory when the subject is far from the target location. Furthermore, to test if these patterns were robust, we also individually applied this cross-decoding analysis to the first and second halves of each session, but we found that decoding performance did not differ between both halves (all p's> 0.05, chi-square test). Overall, these results demonstrate that EC memory-trace cells exhibit a distinctive firing-rate code for individual memory cues that is consistent both during the hold period as well as when the subject moves through the associated target location.

Discussion

A crucial aspect of human memory is our ability to actively target and differentiate past experiences. Here we show that the activity of EC memory-trace cells selectively represents and differentiates between memories from a single environment. Critically, memory-trace cells represent information about locations that subjects had been cued to remember, illustrating how top-down memory demands influence the brain's representation of space. Our observations suggest that memory-trace cell activity represents object locations you are trying to remember. The activity of EC memory-trace cells, specifically, was predictive of the cued memory both during the stationary hold period as well as when subjects moved through retrieved locations, suggesting these cells support a generalizable and robust memory-specific representation. Our findings thus indicate that, in addition to the fixed metric for space provided by grid cells[6,13], the human EC also contains neurons that support a flexible spatial code modulated by top-down memory demands. Below, we discuss how memory-trace cells relate to previous single-cell findings in the hippocampus and EC relevant to space and memory, and how they help explain the broader role of the EC in the brain's memory network.

Place cells in the hippocampus are thought to represent a map of the current environment, and evidence shows that these representations remap in response to changes to the environment[33, 34]. This led to the hypothesis that different environmental contexts induce orthogonal spatial representations in these cells, which are used to index different maps for past experiences[7, 8]. The phenomenon of "goal-oriented" remapping, in which place fields change location and/or accumulate near goal locations without changes to local cues or spatial context, demonstrates that top-down influence and goal-driven behavior can modulate spatial firing[9, 10]. A significant proportion of memory-trace cells exhibited firing fields at different offsets from the response location depending on the cue being retrieved, demonstrating a potential link to goal-oriented remapping and suggesting that the link between remapping and memory-trace cell activity should be further investigated. Furthermore, distal CA1 place cells — which receive direct EC input — show partial remapping based on the presence and location of objects in the environment[35], raising the possibility that EC memory-trace cells also influence or interact with hippocampal remapping. Future work should investigate the relationship between our findings and remapping, and how these phenomena interact in service of memory.

That memory-trace cell activity tracked the current cued memory indicates that subjects' top-down memory retrieval states influenced the firing of these cells. Related work has found cells that represent goal-related spatial information in the hippocampal formation of rodents and bats[11,29,36]. The key distinction between memory-trace cells and these other cell types is that memory-trace cells do not significantly activate when objects, the putative goal, are visible in the environment. As such, memory-trace cell activity likely is more specifically related to memory retrieval processes, rather than goal coding in general. Interestingly, some specific properties of memory-trace cells recapitulate elements of these goal-coding cells. Specifically, goal cells in rodent subiculum also fire in locations preceding rewards[11], and goal representations in bats[29] are also maintained even when the goal is occluded. Additionally, some memory-trace cells exhibited firing fields at fixed offsets from the response location independent of the cue, providing a potential link to hippocampal goal-vector coding. Future work that more extensively measures memory-trace cell activity relative to visible goals may characterize their similarity to goal cells.

Our finding that memory-trace cells in the EC, in particular, exhibited consistently decodable representations of individual object–location memories extends prior work documenting the EC's role in the representation of object features and context in rodents and non-human primates[16, 37]. Specifically, our findings bear significant resemblance to "object-trace cells" discovered in rodent EC[18] and cingulate[38]. Rodent object-trace cells activated in locations where animals had previously encountered objects and could represent a non-specific, putative trace of all the objects that the rodent had encountered in the environment. However, human memory-trace cells had two crucial additional features that were not observed in rodents. The activity of memory-trace cells specifically tracked the location subjects recalled, indicating that subjects' top-down memory target modulated their spatial tuning, rather than showing increased activity for all previous object–locations as in rodent object-trace cells. Additionally, memory-trace cells exhibited a memory-specific rate code even when subjects were not moving through the environment.

This prevalence of memory-trace cells in the EC may advance our understanding of the functional role of the entorhinal region in memory. Recent work using neuromodulation has demonstrated a causal role for the EC in human spatial and episodic memory[39, 40]. Additionally, the EC is thought to be an early staging ground for the onset of Alzheimer's disease[41, 42], with evidence suggesting that the spread of Alzheimer's pathology begins in the EC[43] and that entorhinal tau is directly linked to memory decline in old age[44]. Given these lines of research, one possibility is that the memory-trace cells we identified are affected by stimulation or lesion of the EC, resulting in these subsequent effects on memory. Indeed, recent work has shown that mice expressing tau pathology in EC showed concomitant spatial memory deficits and major loss of cells in EC layers II and III, providing evidence of a potential link between loss of memory-related cells in the EC (such as memory-trace cells) and memory deficits[45].

Additionally, recent work in humans has shown that the activity of grid cells is degraded in people at risk for Alzheimer's[19], and is correlated with spatial memory performance[46,47]. It is possible that grid cells and memory-trace cells both contribute to EC memory circuits, and the relationship between them may be important to understanding how spatial and memory

processes interact in the EC. Indeed, two recent studies in rodents discovered that grid cell maps shift to represent remembered reward locations, suggesting the influence of task-relevant variables on the structure of entorhinal spatial maps[20,48]. Our findings build upon this work by demonstrating a specific way in which top-down processes may interact with flexible spatial representations to index events for memory retrieval in the EC.

We also found a small but significant proportion of memory-trace cells in cingulate cortex in addition to the EC. Our previous work identified grid-like single neuron activity in the cingulate cortex of humans, in addition to the EC[13], complementing related findings from fMRI showing grid representations outside of the EC[46]. The co-localization of memory-trace cells and grid cells suggests that these cells represent a common memory network involving both EC and cingulate cortex. Going forward, further exploration of the relationship between memory-trace cells and grid cells may provide insights into the neural mechanisms underlying spatial and mnemonic function across regions.

In conclusion, we demonstrate the existence of memory-trace cells that flexibly change their spatial tuning to distinguish individual memories during retrieval. EC memory-trace cells exhibited consistent activity across the hold and response periods of our task, allowing us to decode cued memories and indicating that EC representations persist beyond purely spatial or navigational settings. This supports the notion that the EC is important for general relational and contextual memory representations[16, 17]. Looking forward, although our results focus on how memory modulates spatial tuning to distinguish subjective memory representations, other emerging lines of work now show that the EC maps non-spatial features of experience[49, 50]. Our findings may therefore enable new lines of investigation in various species of how entorhinal neuronal representations of space and other domains are modulated by top-down demands in service of memory and other high-level cognitive processes.

Methods

Task.

Nineteen patients with drug-resistant epilepsy performed 31 sessions of a spatial-memory task at their bedside with a laptop computer and handheld controller. This study was approved by the Institutional Review Boards of Columbia University, Columbia University Medical Center, Emory University, University of Texas Southwestern, and Thomas Jefferson University. All subjects provided written consent agreeing to participation in this experiment. In this virtual reality (VR) memory task, subjects are moved from the beginning to the end of a linear track on each trial. The track is 68 VR-units long, which corresponds to approximately 231 meters when converted using the height of the virtual avatar relative to the environment and track length. The ground was textured to mimic asphalt and the track was surrounded by stone walls (Fig. 1a). On each trial subjects are placed at the beginning of the track and shown text cues instructing them to press a button on the game controller when they reach the location of a specified object (“instruction period”). Immediately after receiving this cue, subjects press a button on a game controller to move to the “hold period,” in which they are held stationary at the entrance to the track for 4 seconds. Next, the “movement period” begins automatically, in which subjects are moved forward along the

track. Subjects are moved passively for 56 of 64 trials and on other, randomly selected trials, control movements with a handheld controller (Supplementary Fig. 1a). Individual trials consisted of either encoding or retrieval trials (see Fig. 1a). The first two times that subjects encounter a particular object are encoding trials, in which the object is visible during movement so the subjects can learn its location. On subsequent retrieval trials, the object is invisible and subjects are instructed to recall its location by pressing the controller button when they believe they are at the correct location. To measure task performance, we compute the distance error (DE) on each trial, defined as the distance between the subject's response location and the actual location of the object. Subjects encode and retrieve a total of 4 unique object–location associations (16 trials of each) over the course of a session, with each object located at a different randomly selected location (Fig. 1b). Objects' temporal order and spatial order were randomly associated, such that the each object would be randomly be assigned to locations 1-4 independent of the temporal order of that object (i.e. the 1st object in the session could be presented in the 4th location).

In addition to pressing a button to indicate their memory for the object location, subjects are told to press a button as they enter the "stopping zone" at the end of the track, which is visually delineated by a red floor coloring at the end of the track. Pressing the button in this region ends the movement period, and subjects are then shown a fixation cross for 5 seconds ("fixation period").

Finally, during the "feedback" period at the end of each trial, subjects receive points corresponding to how close to the correct location they pressed the button during movement. Only one object was ever present on the track at any given time. The task was split into two blocks so that subjects would only be cued to retrieve from either the 1st or 2nd object in the first block vs. the 3rd or 4th object for the second block. After learning the location of an object during the encoding trials, subjects were cued with that object for at least two consecutive trials before potentially being cued with the other object for that block (see Supplementary Fig. 1a).

A distinctive feature of our task is that during movement periods subjects are moved passively while their speed is automatically changed in a seemingly random fashion. These uncontrolled speed changes encourage subjects to attend continuously to their current VR location because they cannot accurately predict future positions by integrating their past velocity. Within each third of the track, subjects are moved at a constant speed, which is randomly chosen from the range of 2 to 12 VR units per second. The areas where speed changes occur is indicated in the schematic shown in Figure 1b. When speed changes occur, acceleration occurs gradually over the course of one second to avoid a jarring transition.

Data recording.

The subjects in our study were epilepsy patients who had Behnke-Fried microelectrodes surgically implanted in the course of clinical seizure mapping[51] at four hospital sites: Emory University Hospital (Atlanta, GA), UT Southwestern Medical Center (Dallas, TX), Thomas Jefferson University Hospital (Philadelphia, PA), and Columbia University Medical Center (New York, NY). Microwire implantation and data acquisition largely followed previously reported procedures[13] and were approved by an Institutional Review Board (IRB) at all

participating institutions, and informed consent was obtained from all participants. The depth electrodes feature 9 platinum–iridium microwires (40 μm) extending from the electrode tip and were implanted in target regions selected for clinical purposes. We recorded microwire data at 30 kHz using either the Cheetah (Neuralynx, Tucson, AZ) or NeuroPort (Blackrock Microsystems, Salt Lake City, UT) recording systems. Data collection and analysis were not performed blind to the conditions of the experiments. We used Combinato[52] for spike detection and sorting. We excluded neurons that had a mean firing rate below 0.2 Hz or above 15 Hz (potential interneurons). Manual sorting identified single- vs. multi-unit activity vs. noise on the basis of previously determined criteria[53, 54].

Microelectrode bundle localization followed a similar process as described previously[39, 55]. We determined the anatomic location of each implanted microwire electrode bundle using a combination of pre-implantation magnetic resonance imaging (MRI) and post-implantation computed tomography (CT) scans (Supplementary Fig. 2). First, we performed automated whole brain and medial temporal lobe anatomic segmentation on T1-weighted (whole brain coverage, 3D acquisition, 1mm isotropic resolution) and T2-weighted (temporal lobe coverage, coronal turbo spin echo acquisition, 0.4 × 0.4 × 2 mm resolution) MRI[56, 57]. A post-implantation CT scan was then co-registered to the MRI scans and a neuroradiologist identified the positions of electrode contacts and microwire bundles based on the source images and processed data[58]. Further detail regarding imaging parameters can be found in the Life Sciences Reporting Summary.

Statistical analysis.

No statistical methods were used to pre-determine sample sizes but our sample sizes are similar to those reported in previous publications[13, 59]. For all omnibus testing (ANOVA) described in this study, we used a non-parametric permutation method to generate a large number of permutations where observations are permuted within each block. This enabled us to determine critical statistics and p-values (permutation adjusted) against empirically derived null distributions. Firing rate was z-scored within each session, omitting manual movement trials. Because overall z-scored firing rates may be subject to bias from stimulus-induced increases in firing rate, we computed the z-score after removing the spatial bin with the highest firing rate on each trial or spatial bins with $z > 3.29$ (exceeding the 99.9th percentile of the normal distribution).

Identifying place cells and memory-trace cells.

To examine how neuronal activity varied with location in the virtual environment, we binned the virtual track into 40 bins, referred to as “VR-bins” (equivalent to 1.7 VR-units) enabling us to measure neuronal firing rates in this binned space. For each cell, we counted the spikes in each spatial bin and divided this quantity by the time spent in that bin to yield a firing rate estimate. We smoothed this firing rate estimate on the single-trial level using a Gaussian kernel with a width of 8 VR-bins (±4 VR-bins). We excluded the bins in which subjects spent less than 100 ms over the course of the entire task. This excluded several bins in the stopping zone, because the movement period ended as soon as subjects pressed the button in the stopping zone. We did not analyze data from the manual movement trials for this study.

We used a two-way repeated-measure ANOVA to examine the effects of subject location (1-40 VR-bins), object retrieval cue (1, 2, 3, 4), and their interaction, on the binned firing rate of each cell. After using the ANOVA to screen cell responses, we defined individual spatial firing fields as contiguous bins in which firing rate exceeded a baseline threshold[21,36,60,61]. We determined this baseline threshold independently for each cell, using non-parametric permutation testing to build empirical estimates of the threshold by circularly shifting the firing rate estimates 500 times, re-binning the firing rate, and selecting the 95th percentile of the permuted distribution of firing rates.

We defined place cells as those cells that showed a significant main effect of location on firing rate via the ANOVA, and that also had a spatial firing field (its “place field”) greater than 5% the size of the track. Additionally, we performed an ANCOVA to confirm the main effect of position in the ANOVA, with position serving as a main factor while speed and time were covariates[24]. This analysis used a 3-s window surrounding the response, as anticipatory motor responses occur within 1 s of a movement[30]. We only considered a neuron to be a place cell if its firing was significantly modulated by subject location even after factoring time and speed in as covariates in the ANCOVA. Additionally, six cells showed a main effect of object cue on firing rate. These cells were excluded from analyses. We defined memory-trace cells as those cells whose firing rate showed an interaction between subject location and object cue in the ANOVA and that showed a significant spatial firing field (its “trace field”) for at least one cue. A trace field for a particular object cue was considered unique if the peak location, where firing rate was maximal, did not overlap with that of any other trace field for that cell.

Because all subsequent analyses relied on our characterization of place and memory-trace cells, we conducted a suite of control analyses to ensure that the proportions of cells categorized as such was robust to: dependence between task sessions for individual patients, recordings from seizure-onset zones changes in bin-size for spatial firing-rate estimates, and the statistical assumptions of our omnibus testing. These analyses and their results are summarized in Supplementary Table 2.

Correlation between encoding and retrieval firing rates.

We computed the correlation between the spatial firing patterns of each memory-trace cell between retrieval and encoding trials to establish if memory-trace cells fire in the same locations during these phases at different firing rates (“congruent”) or whether they exhibited completely different firing patterns during these two phases (“incongruent”). Specifically, we limited this analysis to the blocks of trials in which the subject viewed a cue for which a memory-trace cell had a trace field, as these cells had trace fields for 1–4 of the cues. We assessed significance using a permutation procedure, comparing the actual correlation coefficient to the coefficient computed by applying the same procedure to randomly shuffled firing rate vectors. We then tested the significance of the proportion of cue-conditions showing congruent spatial firing between encoding and retrieval trace fields against the proportion showing incongruent spatial firing.

Assay of attention during encoding trials.

We examined the effect of attention[62] on memory-trace cell activity. To assay attention, we relied on the fact that the object is visible during the encoding trials of the task. This visibility ensured that subjects' performance on these trials would depend primarily on how closely the subject was attending to their location in space. We thus utilized subjects; distance error on encoding trials as a proxy measure for attention level. This assay allowed us to examine the putative effect of attention on neural activity independently of memory retrieval. We therefore split encoding trials into low- and high-attention groups, based on whether the distance error between the button press and the visible object was greater or less than 1.5 VR bins, respectively (determined via mean split). We performed a two-way ANOVA assessing how memory-trace cell activity during encoding was modulated by attention level on that trial (low or high) as well as the location of the trace field relative to the response.

Task-period firing rate comparison.

In order to compare the magnitude of pre- vs. post-response firing rate changes to firing rates during different task periods, we computed the "response period" firing rate by normalizing the activity in the 10 VR-bins preceding the response by the 10 VR-bins following the response. This also helped ensure that correlations computed between task periods and the response period (see Fig. 6) were not confounded by trial-wide increases in baseline firing rate. We used robust linear regression to examine the correlation between hold and response period activity (Fig. 6b, c). This approach minimizes the effect of outliers using iteratively re-weighted least squares with a bisquare weighting function[63].

To further verify that some other aspect of our chosen response period was not leading to artifactual correlation, we computed the correlation between the hold period firing rate and a matched "control period". The control period was computed identically to the response period, but we used the regions of the track that did not overlap with the response period. In this way, the control period was of equal length to the response period, and the neural activity during this control period did not overlap with the neural activity during the response period in order to control for the effect of the response on firing rate.

Cross-decoding analysis.

We used a multivariate cross-decoding framework to test whether memory-trace cell activity reflected information about each object–location memory across different retrieval contexts. This framework is schematized in Supplementary Figure 13. To assess cross-decoding performance, we pooled the memory-trace cells recorded across all patients and sessions and constructed two pseudopopulations: EC memory-trace cells and non-entorhinal memory-trace cells. Pseudopopulation decoding has been used to describe the common neural dynamics of functionally similar subsets of cells without the inherent noise correlations shared by neurons recorded in the same session[59]. For each decoder, we used a k-nearest neighbors algorithm using a one-vs.-all paradigm for multi-class decoding of the remembered item from the recorded neuronal activity. Firing rates were binned by task period and normalized. As detailed in the previous section, on each trial we computed the "response period" firing rate by normalizing the activity in the 10 VR-bins preceding the

response by the 10 VR-bins following the response (Supplementary Fig. 13). We computed the response period firing rate for every trial, regardless of response accuracy. We also used a similar method to compute a matched "control period", which was based on the 20 VR-bins that were not used to compute the response period activity.

For cross-decoding, each separate decoder was trained to predict the currently cued object-location memory from the normalized firing rates of the population of memory-trace cells for each of the task periods. Each model was then tested on activity from a different period. In addition to our cross-decoding framework, we trained and tested decoders on the same periods' activity—these decoders were trained using leave-one-out cross validation to assess performance (Supplementary Fig. 13). We assessed significant decoding accuracy using a binomial test. Chance-level decoding accuracy was 25%, as verified by shuffling all labels and reassessing the decoding performance across the 1000 random permutations.

Data availability.

The data that support the findings of this study are available on reasonable request from the corresponding author. The data are not publicly available because they could compromise research participant privacy/consent.

Code availability.

Task was coded using the publicly available programming library PandaEPL[64]. Analysis was performed in Matlab and spike sorting in Python using the publicly available software package Combinato[52]. Analysis code is available on reasonable request from the corresponding author.

Supplementary Material

Refer to Web version on PubMed Central for supplementary material.

Acknowledgments

We are grateful to the patients for participating in our study. This work was supported by NIH grants R01-MH104606 (to J.J.), S10-OD018211 (to C.S.), NSF grants BCS-1724243 and BCS-1848465 (to J.J.), and NSF Graduate Research Fellowship DGE 16-44869 (to S.E.Q.). We thank Andrew Watrous, Melina Tsitsiklis, Ida Momennejad, Mariam Aly, Nicole Long, and Niko Kriegeskorte for helpful comments and suggestions.

References

[1]. Scoville WB & Milner B Loss of recent memory after bilateral hippocampal lesions. Journal of Neurology, Neurosurgreery, and Psychiatry 20, 11–21 (1957).

[2]. Squire LR, Knowlton B & Musen G The structure and organization of memory. Annual Review of Psychology 44, 453–495 (1993).

[3]. O'Keefe J & Nadel L The hippocampus as a cognitive map (Oxford University Press, New York, 1978).

[4]. Buzsaki G & Moser E Memory, navigation and theta rhythm in the hippocampal-entorhinal system. Nature Neuroscience 16, 130–138 (2013). [PubMed: 23354386]

[5]. O'Keefe J & Dostrovsky J The hippocampus as a spatial map: Preliminary evidence from unit activity in the freely-moving rat. Brain Research 34, 171–175 (1971). [PubMed: 5124915]

[6]. Hafting T, Fyhn M, Molden S, Moser M-B & Moser EI Microstructure of a spatial map in the entorhinal cortex. Nature 436, 801–806 (2005). [PubMed: 15965463]

[7]. Leutgeb S, Leutgeb JK, Treves A, Moser M-B & Moser EI Distinct ensemble codes in hippocampal areas ca3 and ca1. Science 305, 1295–1298 (2004). [PubMed: 15272123]

[8]. Colgin L, Moser E & Moser M Understanding memory through hippocampal remapping. Trends in Neurosciences 31, 469–477 (2008). [PubMed: 18687478]

[9]. Markus EJ et al. Interactions between location and task affect the spatial and directional firing of hippocampal neurons. Journal of Neuroscience 15, 7079 (1995). [PubMed: 7472463]

[10]. Dupret D, O'Neill J, Pleydell-Bouverie B & Csicsvari J The reorganization and reactivation of hippocampal maps predict spatial memory performance. Nat Neurosci 13, 995–1002 (2010). [PubMed: 20639874]

[11]. Gauthier JL & Tank DW A dedicated population for reward coding in the hippocampus. Neuron 99, 179–193.e7 (2018). [PubMed: 30008297]

[12]. Sugar J & Moser M-B Episodic memory: Neuronal codes for what, where, and when. Hippocampus (2019).

[13]. Jacobs J et al. Direct recordings of grid-like neuronal activity in human spatial navigation. Nature Neuroscience 16, 1188–1190 (2013). [PubMed: 23912946]

[14]. Brun V et al. Place cells and place recognition maintained by direct entorhinal-hippocampal circuitry. Science 296, 2243 (2002). [PubMed: 12077421]

[15]. Chao OY, Huston JP, Li J-S, Wang A-L & de Souza Silva MA The medial prefrontal cortex-lateral entorhinal cortex circuit is essential for episodic-like memory and associative object-recognition. Hippocampus 26, 633–45 (2016). [PubMed: 26501829]

[16]. Knierim JJ, Neunuebel JP & Deshmukh SS Functional correlates of the lateral and medial entorhinal cortex: objects, path integration and local-global reference frames. Philos Trans R Soc Lond B Biol Sci 369, 20130369 (2014). [PubMed: 24366146]

[17]. Behrens TEJ et al. What is a cognitive map? organizing knowledge for flexible behavior. Neuron 100, 490–509 (2018). [PubMed: 30359611]

[18]. Tsao A, Moser M-B & Moser EI Traces of experience in the lateral entorhinal cortex. Current Biology (2013).

[19]. Kunz L et al. Reduced grid-cell–like representations in adults at genetic risk for alzheimer's disease. Science 350, 430–433 (2015). [PubMed: 26494756]

[20]. Butler WN, Hardcastle K & Giocomo LM Remembered reward locations restructure entorhinal spatial maps. Science 363, 1447–1452 (2019). URL http://science.sciencemag.org/content/363/6434/1447. http://science.sciencemag.org/content/363/6434/1447.full.pdf. [PubMed: 30923222]

[21]. Ekstrom AD et al. Cellular networks underlying human spatial navigation. Nature 425, 184–187 (2003). [PubMed: 12968182]

[22]. Kraus BJ et al. During running in place, grid cells integrate elapsed time and distance run. Neuron 88, 578–589 (2015). [PubMed: 26539893]

[23]. Kropff E, Carmichael JE, Moser M-B & Moser EI Speed cells in the medial entorhinal cortex. Nature 523, 419–24 (2015). [PubMed: 26176924]

[24]. Robitsek R, White J & Eichenbaum H Place cell activation predicts subsequent memory. Behavioural brain research (2013).

[25]. Sakai K & Miyashita Y Neural organization for the long-term memory of paired associates. Nature 354, 152–155 (1991). [PubMed: 1944594]

[26]. O'Keefe J & Speakman A Single unit activity in the rat hippocampus during a spatial memory task. Exp Brain Res 68, 1–27 (1987). [PubMed: 3691688]

[27]. Skaggs WE, McNaughton BL, Gothard KM & Markus EJ An information-theoretic approach to deciphering the hippocampal code In Hanson SJ, Cowan JD & Giles CL (eds.) Advances in neural information processing systems, vol. 5, 1030–1037 (Morgan Kaufmann, San Mateo, CA, 1993).

[28]. Stachenfeld KL, Botvinick MM & Gershman SJ The hippocampus as a predictive map. Nat Neurosci 20, 1643–1653 (2017). [PubMed: 28967910]

[29]. Sarel A, Finkelstein A, Las L & Ulanovsky N Vectorial representation of spatial goals in the hippocampus of bats. Science 355, 176–180 (2017). [PubMed: 28082589]

[30]. Mauritz KH & Wise SP Premotor cortex of the rhesus monkey: neuronal activity in anticipation of predictable environmental events. Exp Brain Res 61, 229–44 (1986). [PubMed: 3948938]

[31]. Theeuwes J, Kramer AF & Irwin DE Attention on our mind: the role of spatial attention in visual working memory. Acta Psychol (Amst) 137, 248–51 (2011). [PubMed: 20637448]

[32]. Kriegeskorte N Pattern-information analysis: from stimulus decoding to computational-model testing. Neuroimage 56, 411–21 (2011). [PubMed: 21281719]

[33]. Muller RU & Kubie JL The effects of changes in the environment on the spatial firing of hippocampal complex-spike cells 7, 1951–1968 (1987).

[34]. Leutgeb S et al. Independent codes for spatial and episodic memory in hippocampal neuronal ensembles. Science 309, 619–623 (2005). [PubMed: 16040709]

[35]. Burke SN et al. The influence of objects on place field expression and size in distal hippocampal ca1. Hippocampus 21, 783–801 (2011). [PubMed: 21365714]

[36]. Hollup S, Molden S, Donnett J, Moser M & Moser E Accumulation of hippocampal place fields at the goal location in an annular watermaze task. Journal of Neuroscience 21, 1635–1644 (2001). [PubMed: 11222654]

[37]. Suzuki WA, Miller EK & Desimone R Object and place memory in the macaque entorhinal cortex 78, 1062–1081 (1997).

[38]. Weible AP, Rowland DC, Pang R & Kentros C Neural correlates of novel object and novel location recognition behavior in the mouse anterior cingulate cortex. J Neurophysiol 102, 2055–68 (2009). [PubMed: 19587319]

[39]. Jacobs J et al. Direct electrical stimulation of the human entorhinal region and hippocampus impairs memory. Neuron 92, 1–8 (2016). [PubMed: 27710782]

[40]. Goyal A et al. Electrical stimulation in hippocampus and entorhinal cortex impairs spatial and temporal memory. Journal of Neuroscience 3049–17 (2018).

[41]. Braak H & Braak E Neuropathological stageing of alzheimer-related changes. Acta Neuropathol 82, 239–59 (1991). [PubMed: 1759558]

[42]. Gomez-Isla T et al. Profound Loss of Layer II Entorhinal Cortex Neurons Occurs in Very Mild Alzheimer's Disease. Journal of Neuroscience 16, 4491 (1996). [PubMed: 8699259]

[43]. Jacobs HIL et al. Structural tract alterations predict downstream tau accumulation in amyloid-positive older individuals. Nat Neurosci 21, 424–431 (2018). [PubMed: 29403032]

[44]. Maass A et al. Entorhinal tau pathology, episodic memory decline, and neurodegeneration in aging. J Neurosci 38, 530–543 (2018). [PubMed: 29192126]

[45]. Fu H et al. Tau pathology induces excitatory neuron loss, grid cell dysfunction, and spatial memory deficits reminiscent of early alzheimer's disease. Neuron 93, 533–541.e5 (2017). [PubMed: 28111080]

[46]. Doeller CF, Barry C & Burgess N Evidence for grid cells in a human memory network. Nature 463, 657–661 (2010). [PubMed: 20090680]

[47]. Maidenbaum S, Miller J, Stein JM & Jacobs J Grid-like hexadirectional modulation of human entorhinal theta oscillations. Proc Natl Acad Sci US A 115, 10798–10803 (2018).

[48]. Boccara CN, Nardin M, Stella F, O'Neill J & Csicsvari J The entorhinal cognitive map is attracted to goals. Science 363, 1443–1447 (2019). URL http://science.sciencemag.org/content/363/6434/1443. http://science.sciencemag.org/content/363/6434/1443.full.pdf. [PubMed: 30923221]

[49]. Constantinescu AO, O'Reilly JX & Behrens TEJ Organizing conceptual knowledge in humans with a gridlike code. Science 352, 1464–1468 (2016). [PubMed: 27313047]

[50]. Aronov D, Nevers R & Tank DW Mapping of a non-spatial dimension by the hippocampal–entorhinal circuit. Nature 543, 719 (2017). [PubMed: 28358077]

[51]. Fried I et al. Cerebral microdialysis combined with single-neuron and electroencephalographic recording in neurosurgical patients. Journal of Neurosurgery 91, 697–705 (1999). [PubMed: 10507396]

[52]. Niediek J, Bostrom J, Elger CE & Mormann F Reliable analysis of single-unit recordings from the human brain under noisy conditions: Tracking neurons over hours. PLoS One 11, e0166598 (2016). [PubMed: 27930664]

[53]. Hill D, Mehta S & Kleinfeld D Quality metrics to accompany spike sorting of extracellular signals. Journal of Neuroscience 31, 8699–8705 (2011). [PubMed: 21677152]

[54]. Valdez AB, Hickman EN, Treiman DM, Smith KA & Steinmetz PN A statistical method for predicting seizure onset zones from human single-neuron recordings. J Neural Eng 10, 016001 (2013). [PubMed: 23220865]

[55]. Lee SA et al. Electrophysiological signatures of spatial boundaries in the human subiculum. Journal of Neuroscience 218040 (2018).

[56]. Wang H et al. Multi-atlas segmentation with joint label fusion. Pattern Analysis and Machine Intelligence, IEEE Transactions on 35, 611–623 (2013).

[57]. Yushkevich PA et al. Automated volumetry and regional thickness analysis of hippocampal subfields and medial temporal cortical structures in mild cognitive impairment. Human Brain Mapping 36, 258–287 (2015). [PubMed: 25181316]

[58]. Avants BB, Epstein CL, Grossman M & Gee JC Symmetric diffeomorphic image registration with cross-correlation: evaluating automated labeling of elderly and neurodegenerative brain. Medical Image Analysis 12, 26–41 (2008). [PubMed: 17659998]

[59]. Kaminski J et al. Persistently active neurons in human medial frontal and medial temporal lobe support working memory. Nat Neurosci 20, 590–601 (2017). [PubMed: 28218914]

[60]. Fyhn M, Molden S, Witter M, Moser E & Moser M Spatial representation in the entorhinal cortex. Science 305, 1258–1264 (2004). [PubMed: 15333832]

[61]. Alme CB et al. Place cells in the hippocampus: eleven maps for eleven rooms. Proc Natl Acad Sci U S A 111, 18428–35 (2014). [PubMed: 25489089]

[62]. Wilming N, Konig P, Konig S & Buffalo EA Entorhinal cortex receptive fields are modulated by spatial attention, even without movement. Elife 7 (2018).

[63]. Holland PW & Welsch RE Robust regression using iteratively reweighted least-squares. Communications in Statistics: Theory and Methods A6, 813–827 (1977).

[64]. Solway A, Miller JF & Kahana MJ PandaEPL: A library for programming spatial navigation experiments. Behavior Research Methods 45, 1293–1312 (2013). [PubMed: 23549683]

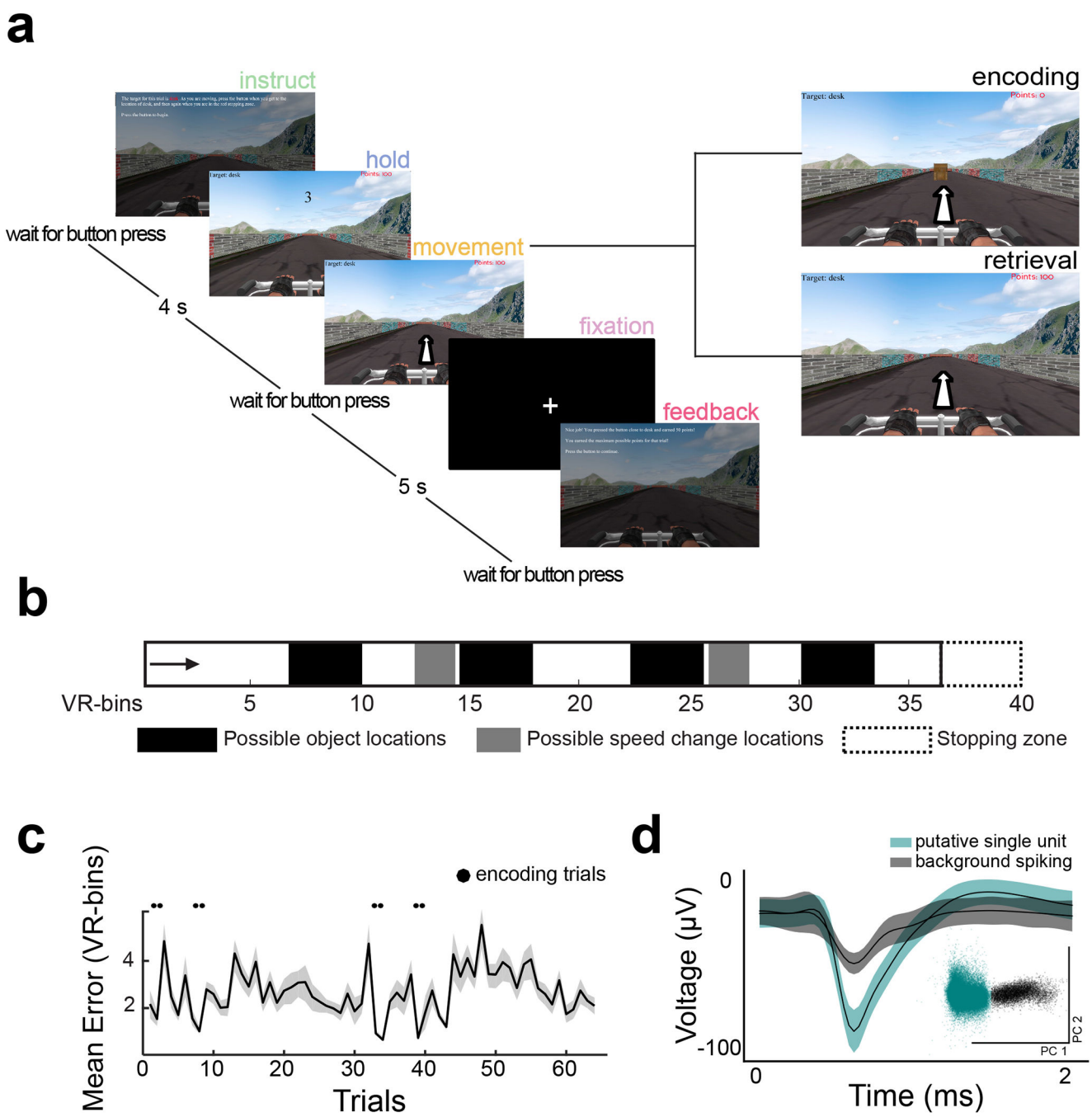

Figure 1: Task overview.

A) Timeline of the object-location memory task. Inset indicates that movement periods either consist of encoding or retrieval epochs. b) An overhead map of the environment. Arrow represents the starting point of each trial. c) Mean response error on retrieval trials, averaged over all task sessions (n = 31 total sessions). Shading indicates standard error (SEM). d) Example putative single-unit waveform (n = 6887 spikes) and example sub-threshold background spiking (n = 78872 spikes). Solid lines indicate mean waveform, shading indicates SEM. Inset shows separation of waveform principal components, whereby

one cluster represents the putative single-unit waveform and the other represents the background spiking.

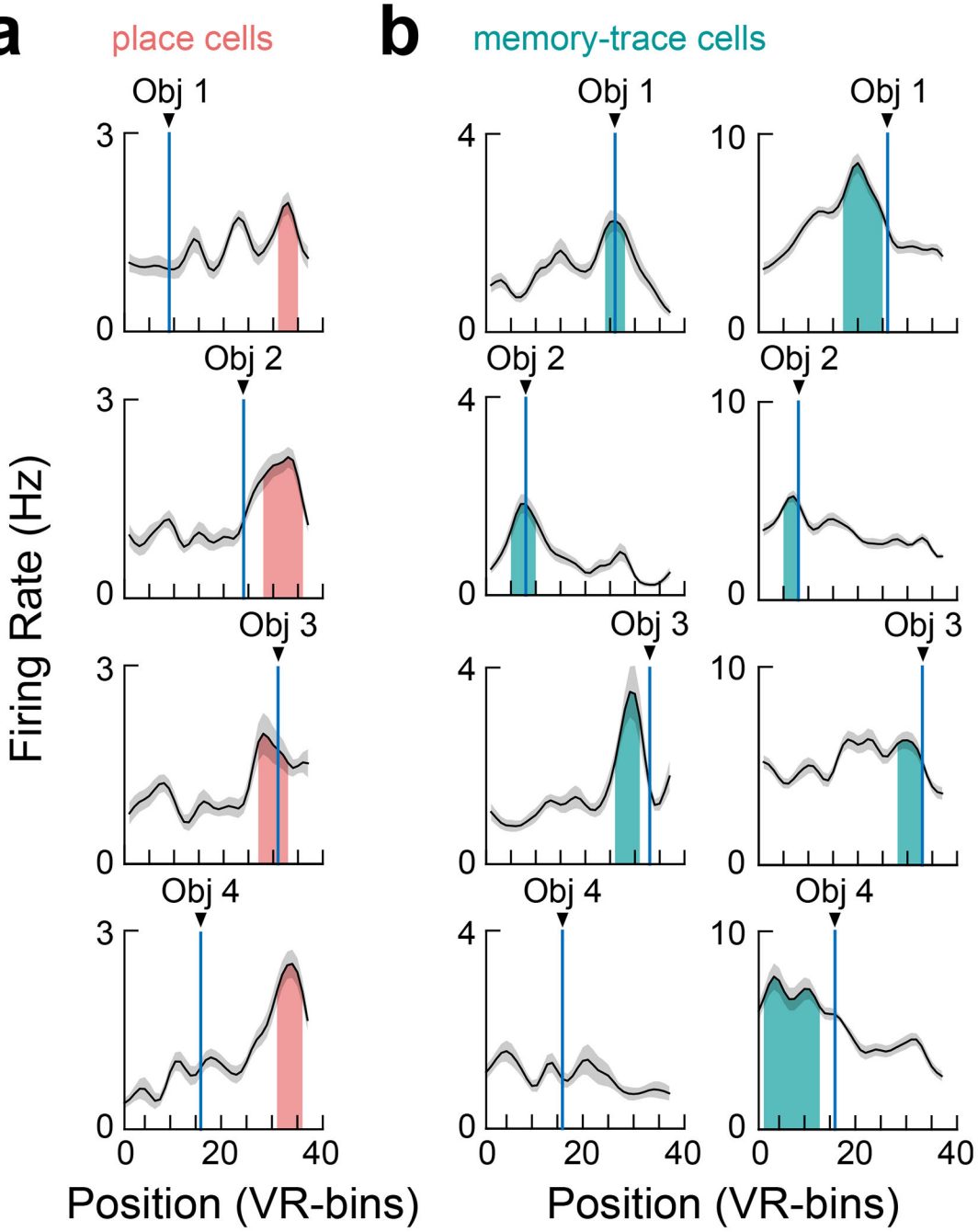

Figure 2: Examples of place and memory-trace cells.

a) The mean firing rate (black lines, $n = 12$ trials per block) of an example hippocampal place cell. Individual plots show this cell's activity for trial blocks with different cue objects. Vertical blue lines indicate object locations. Grey shading indicates SEM. Colored region indicates place fields determined by finding contiguous bins with elevated firing rates (see Methods). b) The activity of two EC memory-trace cells. Note that in contrast to the place cells in panel *A*, these cells' firing fields (shaded regions) shift depending on the retrieval cue.

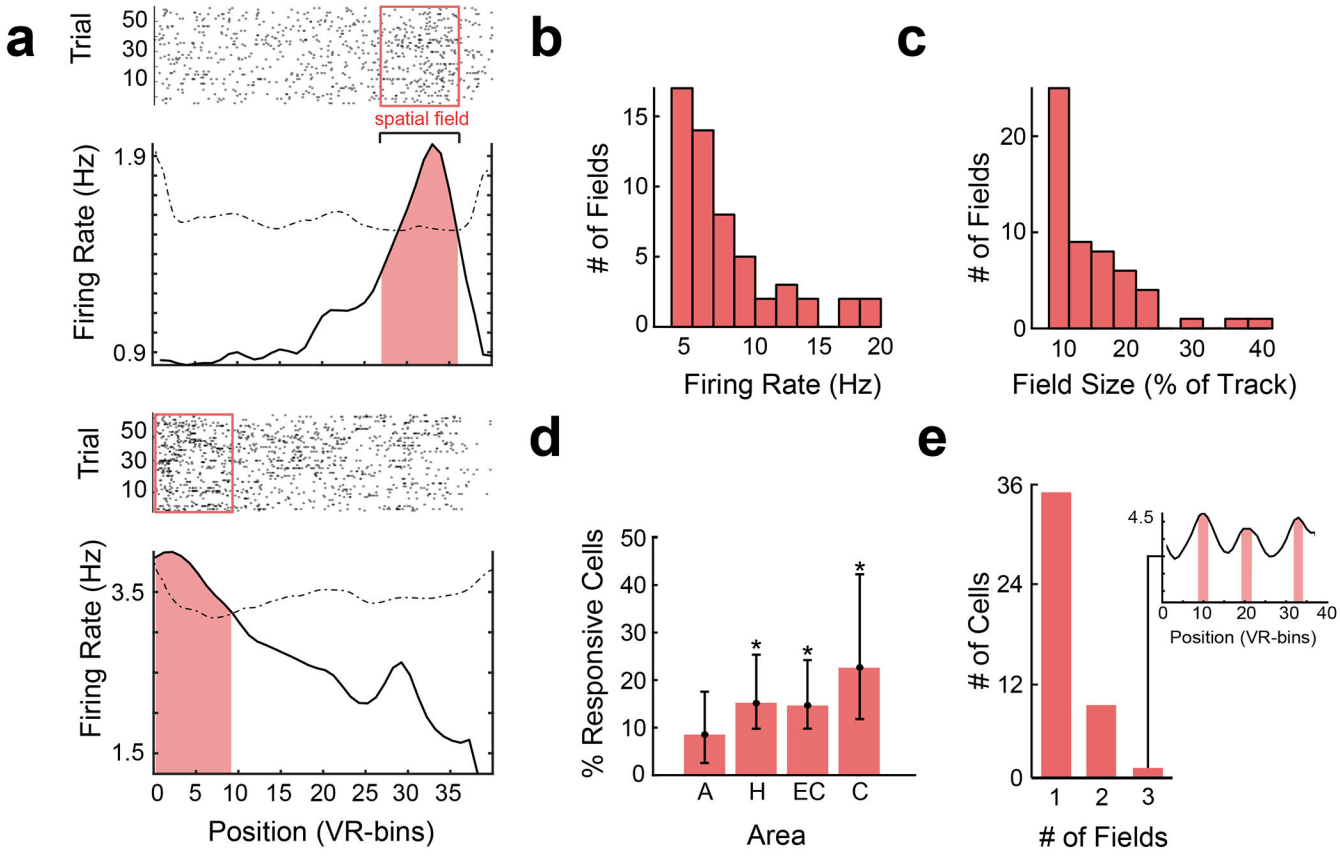

Figure 3: Place cell activity.

a) Raster plot and mean firing rate for two example place cells recorded from the hippocampus. Box and shading indicate place fields. Dotted line represents the threshold for identifying place fields, assessed non-parametrically (see Methods). b) Distribution of mean firing rates among place fields. c) Distribution of field sizes across all place cells, expressed as a percentage of the track. d) Proportion of place cells recorded in each brain area. A = amygdala (n = 62 cells), H = hippocampus (n = 97 cells), EC = entorhinal cortex (n = 113 cells), C = cingulate (n = 27 cells). Asterisks indicate significant proportions (p's< 10^{-4}, two-sided binomial test vs. 5% chance). Error bars indicate the 95% confidence interval from a binomial test. e) Number of responsive cells with more than one spatial field. Inset shows an example cell from the cingulate that showed three spatial fields.

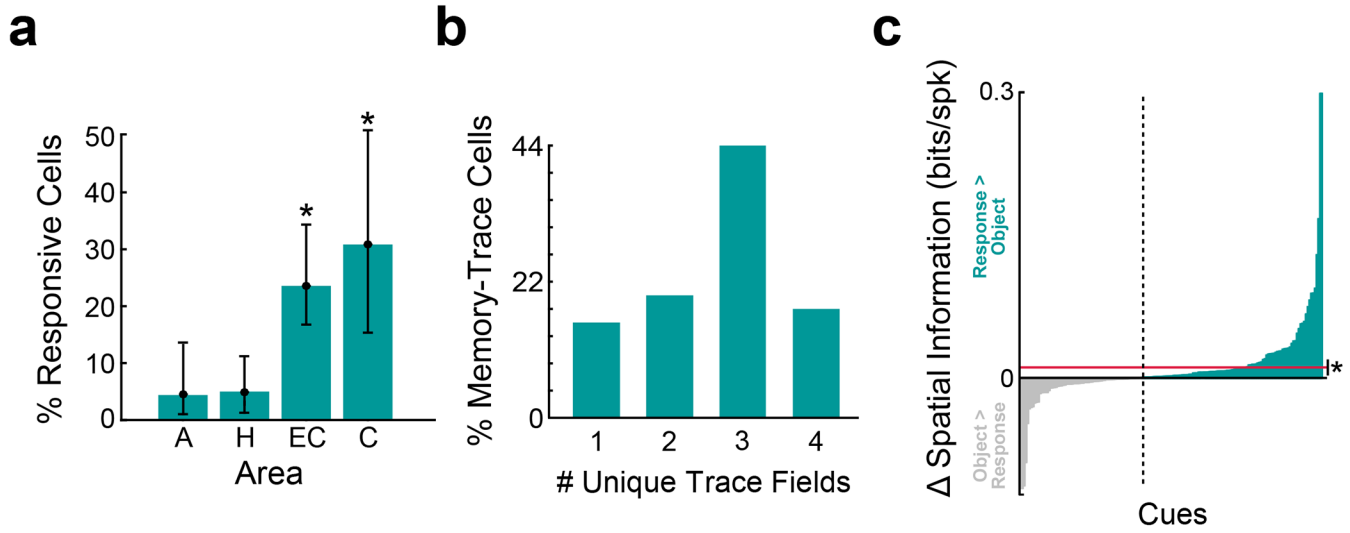

Figure 4: Trace-fields shift according to subjects' memory for cued object locations.

a) Distribution of memory-trace cells across brain areas. A = amygdala (n = 62 cells), H = hippocampus (n = 97 cells), EC = entorhinal cortex (n = 113 cells), C = cingulate (n = 27 cells). Asterisks indicate significant proportions (p's< 10^{-5} two-sided binomial test vs. 5% chance). Error bars indicate the 95% confidence interval from a binomial test. b) Distribution of the counts of unique trace fields exhibited by memory-trace cells. c) Difference in spatial information for each memory-trace cell's firing rate for each cue (n = 168 cues), when aligned relative to response location vs. object location. Asterisk indicates significance (z = 3.4, p = .0007, sign-rank test).

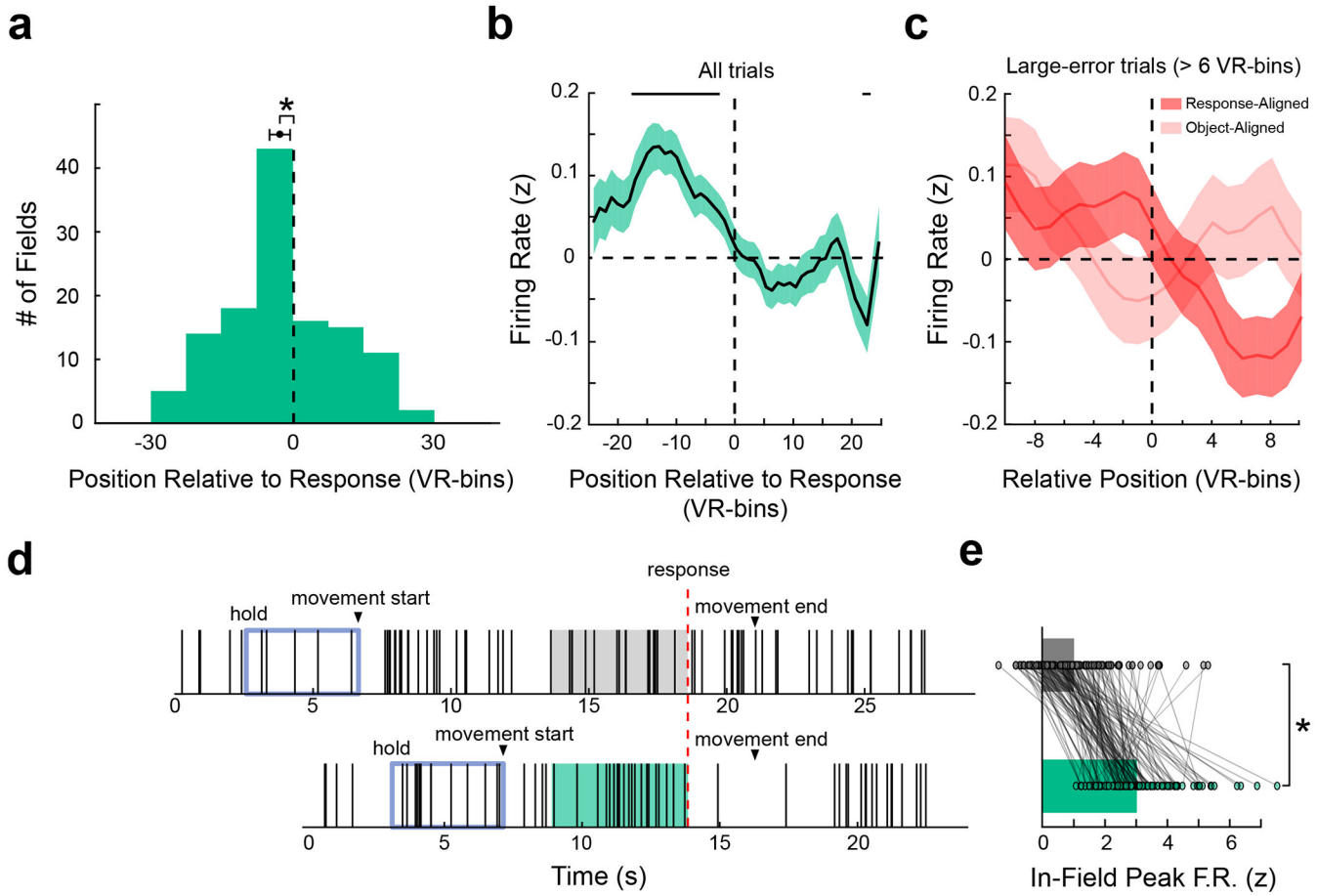

Figure 5: Memory-trace cells track subjective memory during retrieval

a) Distribution of trace-field locations (n = 126 trace fields across 43 memory-trace cells) relative to response location (indicated by black dashed line). Asterisk indicates mean field location significantly precedes response location ($t(125) = 2.09$, $p = 0.038$, two-sided t test). b) Mean firing rate during retrieval trials (z-scored) of all memory-trace cells black line, n = 1990 trials) aligned to response location. Shading indicates SEM. Horizontal lines indicate spatial bins that are significantly different from baseline (p's< 0.05, two-sided t test, FDR-corrected). c) Mean firing rate (z-scored) of all memory-trace cells during large-error trials (solid lines, n = 334 trials), aligned to response location (dark red), or object location (light red). Shading indicates SEM. d) Example spike trains from a single EC memory-trace cell during an example encoding (top) and retrieval (bottom) trial for the same cued location. Vertical lines denote spike times. Responses were aligned and shaded (5 seconds pre-response) to qualitatively illustrate difference in spiking between trial types. e) Population data showing greater memory-trace cell peak firing rate in-field (z-scored) during retrieval than encoding trials, as visualized by the example in panel D ($t(125) = 12.92$, $p = 8.95 \times 10^{-25}$, two-sided t test). Circles denote data from individual trace fields (n = 126).

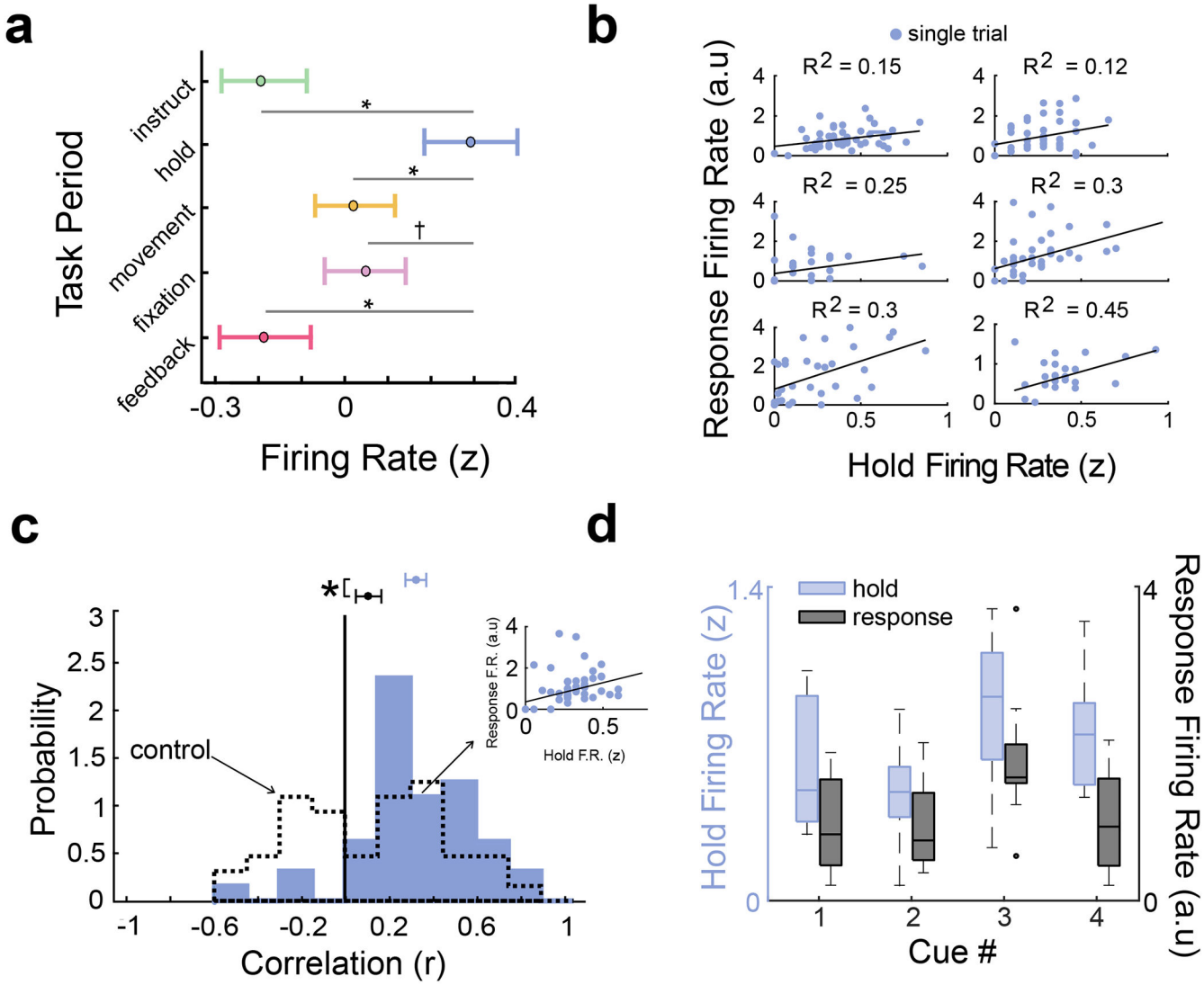

Figure 6: Memory-trace cell activity is correlated between the hold period and response period.

a) Mean normalized (z-scored) firing rate (circles) across all memory-trace cells by task period (n = 1990 trials). Error bars indicate SEM. Asterisks indicate $p < 0.05$ (FDR corrected two-sided t tests); indicates $p < 0.1$. c) Relation of firing rates between hold- and response periods for six example memory-trace cells. Black line denotes the robust linear regression fit. "A.u" denotes arbitrary units, indicating that the response period activity is defined by a ratio (of pre- vs. post-response firing rate). Each plot depicts 48 retrieval trials, excepting the middle-left and bottom-right plots depicting sessions with 24 trials. c) Distribution of Pearson correlation coefficients for memory-trace cell firing rates between hold and response periods (n = 43 cells). Inset shows one example cell's correlation. Circles indicate mean, and error bars indicate SEM. Dotted line denotes control distribution (see Methods). Asterisk indicates significant difference ($t(42) = 2.99$, $p = 0.0046$, two-sided t test). d) Normalized firing rate during hold and response periods for each object cue, for an example EC memory-trace cell. Center line indicates median, box limits indicate

interquartile range (IQR), whiskers indicate 1.5×IQR (n = 12 trials). Circles indicate outliers.

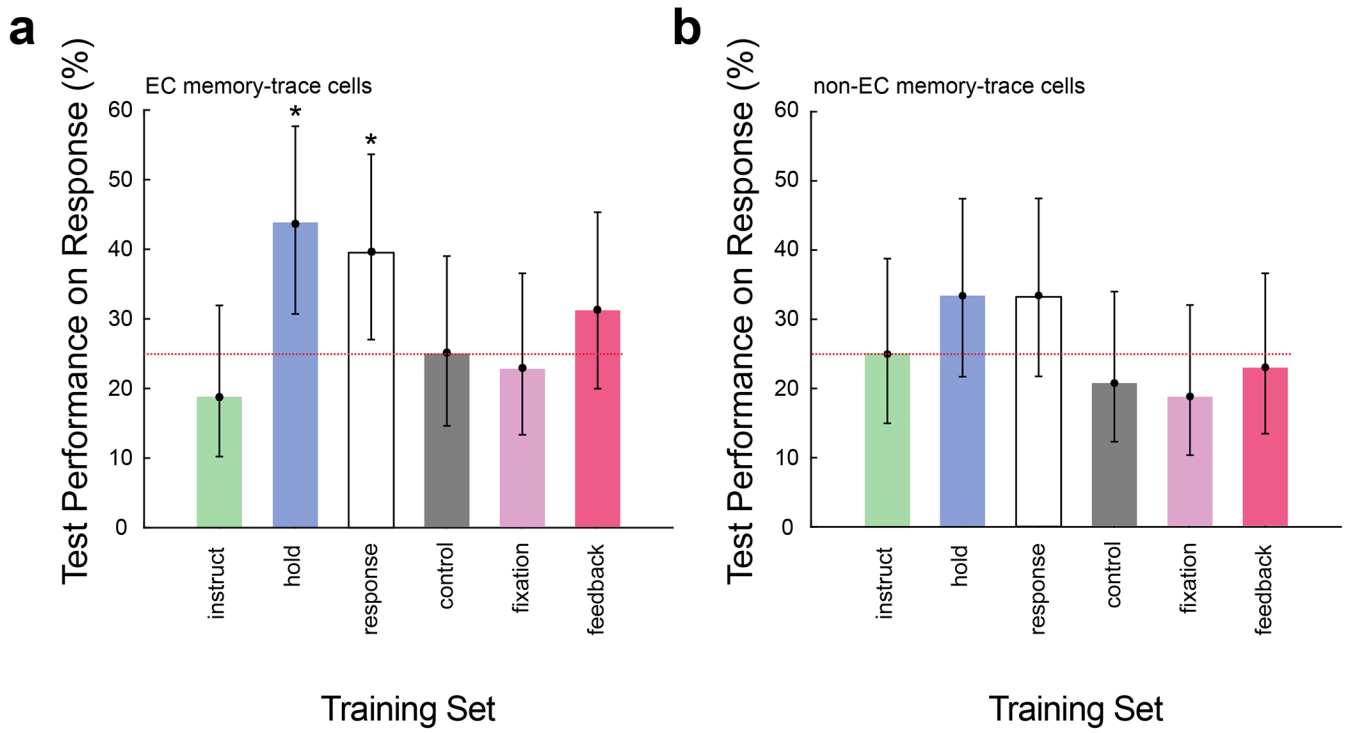

Figure 7: EC memory-trace cell activity predicts cued memory across hold and response periods.

a) Results of memory-decoding analysis for entorhinal cortex memory-trace cells ($n = 27$). Individual bars distinguish models that were trained on different task periods, with all models tested on activity during the response period using trial-level cross validation. Bar height denote testing performance, and error bars indicate the 95% confidence interval from a binomial test. Dotted line indicates chance level performance (25%). Asterisks indicate above-chance decoding accuracy (p's< 0.05, two-sided binomial tests). b) Test performance for decoders based on non-entorhinal cortex memory-trace cell firing ($n = 16$), with training on each of the task periods and testing on the response period.